Novel Approaches to Fast Filling of Hydrogen Cylinders

Pau Miquel Mir

28023668

Supervisor: Dr. Edward Richardson

Word count: 3620

May 2018

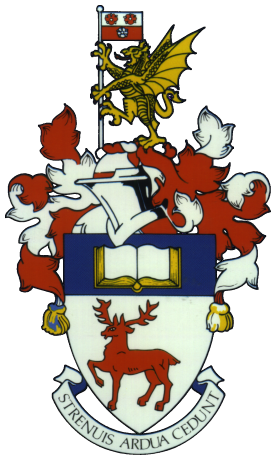

This report is submitted in partial fulfillment of the requirements for the MEng Mechanical Engineering, Faculty of Engineering and the Environment, University of Southampton.

Declaration

I, Pau Miquel Mir, declare that this thesis and the work presented in it are my own and has been generated by me as the result of my own original research. I confirm that:

1. This work was done wholly or mainly while in candidature for a degree at this University;
2. Where any part of this thesis has previously been submitted for any other qualification at this University or any other institution, this has been clearly stated;
3. Where I have consulted the published work of others, this is always clearly attributed;
4. Where I have quoted from the work of others, the source is always given. With the exception of such quotations, this thesis is entirely my own work;
5. I have acknowledged all main sources of help;
6. Where the thesis is based on work done by myself jointly with others, I have made clear exactly what was done by others and what I have contributed myself;
7. None of this work has been published before submission.

Acknowledgements

I want to thank my advisor, Dr. Edward Richardson, for his time, dedication, patience, and support throughout this project.

Furthermore, I would like to thank Vishagen Ramasamy for his initial work upon which this paper builds.

I also want to thank my parents, for their constant support and for proofreading the paper.

Abstract

This is the abstract.

Contents

Acronyms

CFD Computational Fluid Dynamics

ODE Ordinary Differential Equation

Todo list

1 Introduction

{sec:introduction}

1.1 Purpose of the investigation

Hydrogen is a very promising alternative fuel for the future, mainly due to the absence of greenhouse emissions when burning it. In this regard, it is superior to current petroleum- and, more generally, carbon-based fueling systems currently used by most road vehicles. However, air pollution is a negative externality associated with carbon-based fuels, as it is a cost to a third party (in this case, society as a whole) that is not accounted for in the price of the good. By definition, the negative consequences of polluting the air are not accounted for in the price of carbon vehicles, and therefore will have little influence on a consumer's choice. Thus, if hydrogen is to succeed as an alternative to carbon fuels, it is essential that its use be as, if not more, convenient than traditional fuel.

Reword

One of the main aspects where hydrogen currently lags behind traditional fuel is the refueling experience. Given that refueling hydrogen involves its compression, there is a significant rise in temperature, which must be kept below certain standards (358 °K as per SAE J2601). This in turn leads to long refueling times, potentially lasting more than five minutes, which is cumbersome for users. Therefore, it is of prime importance to research and develop systems that enable faster refueling of hydrogen cylinders. To this end, this project builds upon a model of filling a hydrogen cylinder which has already been developed by members of the department to analyse novel methods of improving fill times.

1.2 Outline of the investigation

One of the current solutions to improve fill times involves cooling the hydrogen before filling the cylinder as to keep it below he maximum temperature. However, this is quite expensive, both in energy terms and in economic terms. Consequently, the aim of this project is to continue exploring several of the options available to reduce fill times and simultaneously reduce the energy consumption of the process, thus improving both convenience for users and energy efficiency of the fueling stations. Indeed, by building upon the existing cylinder model several options shall be considered, namely: refrigeration, flow regulation, heat sink usage, active cooling, heat pipe usage, and phase change materials. From here, several options are open to further deepen or potentially broaden the investigation. An attempt to further simplify the model can be made, perhaps even reducing it so a simple algebraic relationship. Also, the model would benefit from FEA validation to aid our understanding of the heat transfer in the structure. This would go hand in hand with analysing the temperature of the structure, and seeing how close this matches the gas temperature. Indeed, if the structure is at a much lower temperature than the gas, the case can be made that the current regulations are slightly erroneous, as they are meant to protect the materials of the structure, but instead regulate the gas temperature.

Update with actual options considered at end of project

reword this crap

2 Background

kground}

2.1 Challenges for compressed hydrogen storage for vehicles

Hydrogen is an attractive alternative fuel because it has zero carbon emissions at point of use. In order to exploit hydrogen on road vehicles it is necessary to have practical hydrogen storage and filling infrastructure. Using liquid storage systems achieves high energy density but requires cryogenic cooling solutions. Metal hydrides are an emerging solution that still needs further development to compete with compressed hydrogen. This study focuses exclusively on compressed gas storage of hydrogen. In order to achieve high energy density very high pressures are required, 35 and 70 MPa being the standards. This hydrogen is then used in the fuel cell and converted into electricity, which can be used directly by the electric motor or stored in onboard batteries. The requirements of a compressed hydrogen system are:

- High fuel capacity
- Low overall weight
- Low fill times

These goals have certain implications. First, it is clear that several tradeoffs and compromises must be made. Increasing fuel capacity can be done by either using larger tanks, which leads to higher weight, or using higher pressures, which inevitably leads to higher temperatures. These higher temperatures are problematic due to material constraints as explained below in Section 2.1.1. Indeed, they lead to longer filling times as heat has to be allowed to dissipate through the tank walls. Thus, solutions must be developed to minimize the temperature rise when filling to high pressures.

havent mentioned temperatures, make link more explicit, joule thompson and compression

2.1.1 Material constraints

The main reason that a problem exists, and consequently this paper (and much other work) is being undertaken, is the material limitations that exist in hydrogen cylinders. Indeed, the cylinders that are used for high pressure scenarios such as the one we are presented with, are constructed with a composite material such as carbon fibre or glass/aramid fibre. In addition, they have a liner that is made out of metal, typically aluminum, in Type III cylinders, and out of a thermoplastic material for Type IV cylinders. Of concern is the composite material, as the polymer matrix cannot withstand high temperatures, and as such the material properties of the cylinder will begin to degrade. The specific temperature at which this occurs is usually around the glass transition temperature of the epoxy, where the thermosetting polymer changes from a hard ”glassy” state to a more compliant ”rubbery” state.

{sec:materialConstr

reword shitty paragraph

cite: http://www.epotek

2.2 Previous work

This section begins with a summary of previous work concerning heat transfer during fast filling of hydrogen cylinders and concludes with an analysis for the need for more research.

2.2.1 Experimental work

{sec:experimental_work}

Several papers describe experimental work that has been conducted regarding the fast-filling of hydrogen cylinders, in particular comparing the results to simulations. Dicken and Mérida's work indicates that the temperature inside the cylinder is rather uniform [1]. This claim is not, however supported by the work of Zheng et al [2] nor that of Woodfield et al [3], wherein large discrepancies among gas temperatures in different regions of the cylinder are found.

2.2.2 Modeling Work

{sec:modelingWork}

Computational Fluid Dynamics (CFD) A large amount of research has been conducted using multidimensional analysis, especially using CFD. Indeed, there are many papers describing different methods and setups, such as Dicken and Mérida's work, which uses the standard k-ε turbulence model and the Redlich-Kwong real gas equation of state for real gas properties [4]. Other investigations use more advanced property models, such as the one presented by Zhao et al., which employs REFPROP (see Section 2.5.3) in order to have more precise real gas properties [5].

Zonal simulations Less work has been conducted regarding reduced order simulations, which employ assumptions such as axisymmetry or uniform gas temperature.

Woodfield et al [3] coupled a single zone model of the gas in the cylinder with a one dimensional unsteady model for the heat conduction through the cylinder walls. They used the Lee-Kesler method [6] to find the compressibility and thus the density and from that the mass inside the cylinder.The heat transfer coefficient between the gas and the wall was assumed to be constant: 500 W/(m^{2}K) during filling and 250 W/(m^{2}K) after full.

double check if true

Similarly, the work by Monde et al [7] uses the same assumption regarding heat transfer coefficient values. They achieve a reasonable fit with experimental data, shown in Fig. 1, even though the measured heat transfer coefficients were significantly lower, shown in Table 1.

FIGURE 1: Comparison between estimated and measured temperatures by Monde et al [7]

{fig:mondeFit}

P (MPa)		Mass flow rate (g/min)	h (W/(m^{2}K))
5	H_2	168 - 276	86.4 - 97.4
	N_2	456 - 1296	43.0 - 47.0
10	H_2	240 - 324	143.1 - 154.5
	N_2	732 - 996	38.9 - 44.7
35	H_2	45-170	269.7 - 279.2

TABLE 1: Heat transfer coefficents at various conditions by Monde et al [7]

{tab:mondeHValues}

2.2.3 Analysis

The simulation work that has been conducted can be, in broad terms, divided into complex CFD models and more simplified reduced dimensional models. It is important to analyze the difference between these two systems.

CFD models have several advantages, as they take into consideration many things which reduced order models must simplify, neglect or assume. Firstly, one can represent the specific effects of geometry of the cylinder more accurately using CFD. Secondly, time effects can be directly simulated without the need of timescales to be modelled. However, they are extremely computationally expensive, with run times lasting from hours to weeks. It thus follows that the main advantage of reduced dimension models is that they are much less computationally expensive. This, in turn, means they can be incorporated as a part of larger analyses, in which they must be run multiple times, such as optimization routines or probabilistic whole station models.

never mentioned before

Reduced dimension models up to date make assumptions that are difficult to support with evidence, and therefore lead to results not being very accurate. This leads to adjustments being made to the model to match the experimental data from the same experiment, which produces a better fit for the model, but leads to a less predictive model. For this reason, it is important to improve reduced order models by devising ways to calculate quantities previously assumed. This will improve the models' predictive ability, which will increase confidence in results from simulations regarding events which haven't been tried experimentally.

do I have evidence

For instance, they assume a homogenous gas temperature, which, as outlined in Section 2.2.1, is supported by some experimental work, but refuted by others. For this reason, more research should be conducted to validate the uniform gas temperature approximation. Another assumption typically made is a constant heat transfer coefficient derived from time-averaged experimental results, as explained in Section 2.2.2. This report will propose a new method of deriving the heat transfer coefficient numerically to achieve better results.

who is they

2.3 Cylinder filling models

Several ways of modelling the cylinder can be considered when analysing their filling, with varying complexity and accuracy.

2.3.1 Zonal

A zonal model, also referred to as a 0-dimensional or reduced order model, refers to models that consider the gas inside the cylinder as the control volume, with homogenous properties. This allows for simpler calculations and much lower computational time.

Fill

2.3.2 Multidimensional

{sec:multidimensior

More complex multidimensional models can be created, either 2D axisymmetric models or full 3D models. 2D models will not include the effects of gravity or buoyancy, but these can be considered

negligible, and the computational expense of full 3D simulations is rarely justifiable as the gains in accuracy are very small.

fill

turbulent jet sis fluid mechanics not heat transfer, rename to physicsy stuff or soemthing?

2.4 Heat transfer models

In order to successfully analyse the behaviour of the system as a whole we must consider several local heat transfer methods that occur at different places inside of the cylinder.

2.4.1 Impinging jet

The first behaviour that we will consider is that of an impinging jet of fluid onto a surface.

FIGURE 2: Impinging jet

{fig:inpinging_jet}

2.4.2 Pipe flow

A second behaviour that we will consider is that of pipe flow. This behaviour has been the focus of much research, as it is arguably the most common mode of heat transfer that occurs in fluid systems.

2.4.3 Turbulent Jets

{sec:turbulentJets}

We must also consider turbulent jets, as the main driver of flow in the cylinder, which in turn drives convective heat transfer, is the turbulent jet that develops from the end of the nozzle throughout the length of the cylinder. Experimental results can be used to derive expressions for the axial velocity of the jet. Radial profiles of mean axial velocity can be seen in Fig. 3.

FIGURE 3: Radial profiles of mean axial velocity in a turbulent round jet with Re = 95,000. Adapted from [8] with the data from [9]

{fig:radialProfile}

By plotting the inverse of the non-dimensional speed, $u_{exit}/u(x)$ against x/d we get the clearly linear relationship shown in Fig. 4.

FIGURE 4: Jet speed vs distance. Adapted from [8] with the data from [9]

{fig:jetSpeed}

From this experimental result the following relationship is obtained:

{{equ:axialSpeed}}

$$\frac{u(x)}{u_{exit}} = \frac{c_1}{(x - x_0)/d_{inlet}} \tag{2.1}$$

where $u(x)$ is the axial velocity at a distance x from the nozzle, x_0 is the position of the virtual origin, and c_1 is an empirical constant.

2.5 Methodology

Several techniques and methods will be used throughout the analysis. These are described in this section.

2.5.1 Optimization

Fill Section once work on optimization starts.

2.5.2 Non-dimensioning

One of the fundamental principles used throughout this paper, and indeed, throughout engineering, is that of non-dimensioning. By operating using non-dimensional parameters such as the Reynolds number $\mathrm{Re} = \frac{\rho u L}{v}$ or the Prandtl number $\mathrm{Pr} = \frac{c_p \mu}{k}$ solving problems involving differential equations becomes simplified. Also, the analysis becomes much more general, and can be scaled.

2.5.3 Numerical methods

{sec:numerical_meth

Integrating Ordinary Differential Equations (ODEs) A central part of solving unsteady heat transfer problems involves integrating ODEs, as will be seen in Section 3. One of the simplest methods available, both conceptually and in terms of ease of implementing in code, is forward Euler time integration. It can be described as follows: given a function that can be defined by:

$$y'(t) = f(t, y(t)), \quad y(t_0) = y_0 \tag{2.2}$$

we can compute the approximate shape of the function given the initial point and finding the slope of the curve for small intervals. Indeed, from the initial point, we can find the tangent of the curve at that point, and take a small step along that tangent until arriving at the next point, where the procedure can be repeated. Denoting the step size as h, we can express forward Euler time integration as:

$$y_{n+1} = y_n + h f(t_n, y_n) \tag{2.3}$$

{sec:property_model

Property models As the gases that are being treated in this report are at very high pressures, ideal gas approximations are inaccurate, and thus real gas properties must be employed. To this end, property models must be used, which can determine any gas property from two other independent properties.

The property model that will be employed throughout this analysis is REFPROP, a tool developed by the National Institute of Standards and Technology [10]. It uses values of critical and triple points together with equations for the thermodynamic and transport properties to calculate the state points of fluids.

3 Formulation

{sec:for

3.1 Governing equation

The governing equation for mass and internal energy of the gas in the tank is given by:

$$\frac{dU_{gas}}{dt} = \frac{d\left(m_{gas}u_{gas}\right)}{dt} = h_{in}\dot{m}_{in} - \dot{Q}_{out} \tag{3.1}$$

consistent time derivatives

where U_{gas} is the total internal energy of the gas, m_{gas} is the mass of the gas, u_{gas} is the specific internal energy of the gas, H_in is the enthalpy of the inlet gas, $\dot{m}_{in}$ the mass flow into the cylinder, and $\dot{Q}_{out}$ is the rate of heat transfer out of the gas to the cylinder.

The change in internal energy of the gas is equal to the difference in energy entering the system in the enthalpy of gas inflow and the energy leaving the system through the walls of the cylinder. The enthalpy of the inlet can be determined from real gas models as a function of the inlet pressure and temperature. Therefore, to obtain the internal energy variation one must calculate the gas mass flow and the heat transferred to the cylinder.

3.2 Gas mass flow into cylinder

The nozzle and corresponding gas flow will be modeled using isentropic relations, and then a discharge coefficient relationship will be used to find the approximate real values. Indeed, the isentropic Reynold's number is first calculated as follows:

equ:reynoldsIdeal}}

$$\mathrm{Re}_{\mathrm{ideal}} = \frac{\rho_{exit}\, d_{inlet}\, u_{exit}}{\mu_{exit}} \tag{3.2}$$

where d_{inlet} is the diameter of the inlet delivery pipe and ρ_{exit}, u_{exit}, and μ_{exit} are determined using real gas models as described in Section 2.5.3. More specifically:

$$\rho_{exit} = f\left(P_{exit}, S_{in}\right), \quad u_{exit} = \sqrt{2\left(H_{in} - H_{static}\right)}, \quad \mu_{exit} = f\left(P_{exit}, S_{in}\right) \tag{3.3}$$

where P_{exit} is the pressure at the end of the inlet tube, S_{in} is the entropy at the inlet, H_{in} the stagnation enthalpy at the inlet, H_{static} the static enthalpy at the end of the inlet tube. As the system is treated as isentropic, the inlet entropy can be used to calculate exit properties. We also have:

$$S_{in} = f\left(P_{in}, T_{in}\right), \quad H_{in} = f\left(P_{in}, T_{in}\right), \quad H_{static} = f\left(P_{exit}, S_{in}\right) \tag{3.4}$$

where P_{in} and T_{in} are the inlet pressure and temperature, respectively. The exit pressure P_{exit} is taken to be the pressure inside the gas tank. However, in the case that the inlet diameter is choked, these calculations would yield velocities higher than the speed of sound, which is impossible due to the nature of the inlet pipe. For this reason, if a velocity of Mach 1 or higher is achieved at any given time, an iterative process is used to find the value of P_{exit} that will yield a velocity equal to the speed of sound, and the rest of properties and ultimately the Reynolds number calculated accordingly.

In order to find the real mass flow an empirical discharge coefficient is employed.

$$C_D = \frac{\dot{m}_{in}}{\dot{m}_{ideal}} = c_2 + c_3 \,\mathrm{Re}_{ideal} \tag{3.5}$$

A discharge coefficient must be used to account for the formation of a boundary layer inside the inlet tube. The empirical model that was used was obtained from , and uses the following values:

Citation

$$c_2 = 0.938, \quad c_3 = -2.71 \tag{3.6}$$

From the real mass flow the actual Reynold's number of the inflow can be calculated and used to find forced convection heat transfer coefficients in Section 3.3.1 and Eq. (3.11) as follows:

avoid forward references

$$\mathrm{Re} = \frac{4\dot{m}_{in}}{\pi \mu d} \tag{3.7}$$

3.3 Heat transfer from gas to cylinder

The heat transferred from the gas to the wall of the tank is given by a simple convection relationship:

$$\dot{Q} = hA\,(T_{gas} - T_{wall}) \tag{3.8}$$ {{equ:convection}}

where A is the internal surface area of the cylinder, h is the heat transfer coefficient, and T_{gas} and T_{wall} are the temperatures of the gas and the wall, respectively. The heat transfer coefficient is a result of the combination of both forced and natural convection. This is expressed as follows, as per [11] and [12]:

$$h = \sqrt[4]{h_f^4 + h_n^4} \tag{3.9}$$

where h_f is the heat transfer coefficient due to forced convection and h_n is the heat transfer coefficient due to natural convection. Each coefficient can be non-dimensionalised using Nusselt's numbers, expressed as:

$$\mathrm{Nu}_f = \frac{h_f D}{k}, \quad \mathrm{Nu}_n = \frac{h_n D}{k} \tag{3.10}$$

where D is the characteristic length, in this case the diameter of the cylinder, and k, the thermal conductivity of the fluid. The values of the Nusselt's numbers can be determined from empirical correlations, as detailed in Sections 3.3.1 and 3.3.2.

3.3.1 Forced convection

{sec:forcedConvecti

As the magnitude of heat transfer is related to the flow in forced convection, the Nusselt's number can be said to be a function of the Reynolds number, taking the form:

$$\mathrm{Nu}_{f,ss} = c_4 \mathrm{Re}^{c_5} \tag{3.11}$$ {{equ:nusseltReynol

where $Nu_{f,ss}$ is the steady state Nusselt's number and the empirical constants c_4 and c_5 are given by as:

cite

eltReynoldsConsts}}

$$c_4 =, \quad c_5 = \tag{3.12}$$

The initial work this project builds upon uses the flow at the nozzle to determine the heat transfer at the wall of the cylinder. This assumes that the hydrogen flows instantaneously from the nozzle to the wall, when in reality there is of course a time delay. This assumption is acceptable for stable inflows, hence us referring to the steady state Nusselt's number $Nu_{f,ss}$, but for more complex filling patterns and also for improved accuracy it becomes necessary to incorporate hysteresis. Indeed, the heat transfer coefficient at the wall in fact can be said to depend on the nozzle flow seconds prior, or more generally, on the history of the nozzle flow. This can be modeled as follows:

Does this need to be cited / proved? Eplain better so you dont have to cite it

$$\frac{d}{dt}\left(\mathrm{Nu}_f\right) = \frac{\mathrm{Nu}_{f,ss} - \mathrm{Nu}_f}{\tau} \tag{3.13}$$

where τ is the time scale, which reflects the amount of time it takes for the flow to recirculate. Two time scales are considered, as two different situations may be present. The flow in the cylinder may be driven by the inflow of mass from the nozzle, in which case we have a time scale of production τ_{prod}. However, if the inflow halts, the flow field in the cylinder will be driven by the dissipation of the existing flow and thus the time scale is denoted τ_{diss}. Therefore the overall time scale is given by the minimum of these two:

explain why it's minimum

$$\tau = \min\left(\tau_{prod}, \tau_{diss}\right) \tag{3.14}$$

The production time scale is given by the spatial integral of the axial speed of the jet, which is given in Eq. (2.1) in Section 2.4.3.

$$\begin{aligned} \tau_{prod} &= \int_0^L \frac{1}{u(x)} dx = \frac{1}{c_1 u_{exit}} \int_0^L (x - x_0)\, dx \\ &= \frac{\frac{L^2}{2} - x_0 L}{c_1 d u_{exit}} \end{aligned} \tag{3.15}$$

As we have $x_0 \ll L$ we can write:

$$\tau_{prod} = \frac{L^2}{2 c_1 d u_{exit}} \tag{3.16}$$

and defining $c_6 = \frac{1}{2c_1}$:

$$\tau_{prod} = c_6 \frac{L^2}{u_{exit} d} \tag{3.17}$$

The dissipation time scale can be said to be proportional to the length of the cylinder L and the recirculation velocity u_{recirc}:

need to explain why?

$$\tau_{diss} = c_7 \frac{L}{u_{recirc}} \tag{3.18}$$

Let us assume that instantaneous Nusselt's number depends on u_{recirc} as it depends on Re^{c_5} and $c_5 \sim \mathscr{O}(1)$. From Eq. (3.11) we know that:

$$\frac{D u_{recirc}}{\nu} = c_8 \mathrm{Nu}_f \tag{3.19}$$

We can therefore rewrite:

$$\tau_{diss} = \frac{c_7}{c_8} \frac{LD}{\nu \mathrm{Nu}_f} \tag{3.20}$$

Combining the two constants and absorbing the L/D coefficient:

$$\tau_{diss} = c_9 \frac{L^2}{\nu \mathrm{Nu}_f} \tag{3.21}$$

We can then make use of the fact that in steady state we know $\tau_{prod} = \tau_{diss}$, which leads to:

$$\tau_{diss} = c_9 \frac{L^2}{\nu \mathrm{Nu}_f} = c_6 \frac{L^2}{u_{exit} d} \tag{3.22}$$

Substituting the definitions of Nusselt's and Reynolds numbers from Eqs. (3.2) and (3.11):

$$c_9 = c_6 \frac{\nu \mathrm{Nu}_f}{u_{exit} d} = c_4 c_6 \tag{3.23}$$

Which leads to a final definition of τ_{diss} in terms of literature constants:

$$\tau_{diss} = \frac{c_4}{2c_1} \frac{L^2}{\nu \mathrm{Nu}_f} \tag{3.24}$$

Therefore, in a pure dissipation scenario, where $\mathrm{Nu}_{f,ss} \to 0$, we have:

$$\frac{d}{dt}\left(\mathrm{Nu}_f\right) = -\mathrm{Nu}_f^2 \frac{2c_1}{c_4} \frac{\nu}{LD} \tag{3.25}$$

Thus, when the inflow stops the heat transfer at the wall will decrease quadratically.

3.3.2 Natural convection

{sec:naturalConvect

Natural convection is caused by buoyancy driven flow, so the natural Nusselt's number can be found to be related to the Rayleigh's number (itself a product of Grashof's and Prandt's numbers) by the following relationship:

$$\mathrm{Nu}_n = c_{10} \mathrm{Ra}^{c_{11}} \tag{3.26}$$

where Rayleigh's number is defined as:

$$\mathrm{Ra} = \left| \frac{g\beta \left(T_{wall} - T_{gas}\right) D^3}{\nu\alpha} \right| \tag{3.27}$$

where g is the acceleration due to gravity, β is the coefficient of thermal expansion, D is the characteristic length, in this case the cylinder diameter, ν is the kinematic viscosity, and α is the thermal diffusivity, as defined by:

hermalDiffusivity}}

$$\alpha = \frac{k}{\rho c} \tag{3.28}$$

where k is the material's thermal conductivity, ρ is the density of the material, and c is the specific heat capacity of the material. The coefficients are given by :

cite

$$c_{10} =, \quad c_{11} = \tag{3.29}$$

3.4 Heat transfer across cylinder

The main mode of heat transfer that occurs in the cylinder and that will be used throughout this report is heat conduction through the wall of the cylinder. This is modeled using:

$$\frac{\partial T}{\partial t} = \alpha \frac{\partial^2 T}{\partial x^2} \tag{3.30}$$

where α is the thermal diffusivity, as defined in Eq. (3.28). This differential equation will be solved using forward Euler time integration as described in Section 2.5.3. Solving this equation will yield the temperature distribution throughout the thickness of the cylinder wall, and more specifically, the internal wall temperature that is used to calculate the heat transferred out of the gas in Eq. (3.8).

3.4.1 Discretization

3.4.2 Outer Wall

3.5 Throttling

Throttling is introduced in order to more accurately represent real life conditions. When a maximum temperature is reached, the inflow of hydrogen must be stopped in order to protect the materials of the tank, as detailed in Section 2.1.1. A simple method of throttling, with the flow stopping at the designated maximum temperature, 85 °C, and the flow restarting at a chosen temperature. The optimum temperature at which flow restarts was considered in this study, and results are presentedl in **??**

3.6 Optimization

General stuff:
- Check tense and person
- Check for repetition
- Check for excessive verboseness - define

4 Results and Discussion

{sec:results}

5 Conclusion

{sec:conclusion}

This is the conclusion.

Appendices

A Filling Code

{app:filling_code}

```
%Author: Vishagen Ramasamy
%Date: -

% Copyright University of Southampton 2017.
% No warranty either expressed or implied is given to the results produced
% by this software.  Neither the University, students or its employees
%accept any responsibility for use of or reliance on results produced by
%this software.

%% script that computes the filling of the tank(s)
%% Importing the pressure and temperature profile at the entrance of the delivery pipe from Dicken a
%  and calulating the stagnation enthalpy and entropy

for j = 1:maxt
    time(j+1) = (j)*dt;                                                          % Time as filling proce
    for i = 1:tank_number
        % Select inlet pressure / temperature profile based on user input
        if blnUseStandardData == 1
            % Constant inlet pressure profile
            P_inlet(i,j+1) = ConstPressKPa;
        else
            % Read inlet pressure profile from specified file
            P_inlet(i, j+1) = interp1(InletPressureData(:,1),InletPressureData(:,3), dt*j);
        end

        if blnUseStandardData == 1
            %Temp_inlet(i,j+1) = interp1(time_in, temp_in, dt*j);   % Temperature profile after the
            Temp_inlet(i, j+1) = ConstTempK;
        else
            % Read inlet temperature profile from specified file
            Temp_inlet(i, j+1) = interp1(InletTempData(:,1), InletTempData(:,3), dt*j);
        end

        h_inlet(i,j+1) = refpropm('H','T',Temp_inlet(i,j+1),'P',P_inlet(i,j+1),Fluid{i}, refpropdir)
        entropy_inlet(i,j+1) = refpropm('S','T',Temp_inlet(i,j+1),'P',P_inlet(i,j+1),Fluid{i}, refpr

        %% Determine which pressure to use at the exit of the delivery pipe which is dependent upon

        if l_d(i) > 3 && blnOneZone{i} == 0          % The length-to-diameter ratio of the tank(s) d
            Pressure_exit = P_gas_zone1{i}(j);   % The pressure at the exit of the delivery pipe is
        else
            Pressure_exit = P_gas(i,j);          % The pressure at the exit of the delivery pipe is
        end

        if (P_inlet(i,j+1) > Pressure_exit)  % condition for filling of tank(s)
            sound_exit(i,j+1) = refpropm('A','P',Pressure_exit,'S',entropy_inlet(i,j+1),Fluid{i}, re
            h_static_exit(i,j+1) = refpropm('H','P',Pressure_exit,'S',entropy_inlet(i,j+1),Fluid{i},
            visc_exit(i,j+1) = refpropm('V','P',Pressure_exit,'S',entropy_inlet(i,j+1),Fluid{i}, ref
            mach_exit(i,j+1) = sqrt(2*(h_inlet(i,j+1)-h_static_exit(i,j+1))/sound_exit(i,j+1)^2);

            %% If Mach number is greater than one, the exit pressure is greater than the pressure wi
            %  is incremetally increased and iterated in a while loop  until mach number is equal to

            Inlet_entropy = entropy_inlet(i,j+1);
            Inlet_stagnation_enthalpy = h_inlet(i,j+1);
            P_guess =  Pressure_exit;

            if mach_exit(i,j+1) > 1
                Pressure_exit = find_exit_pressure(Inlet_stagnation_enthalpy,Inlet_entropy,Fluid{i},
                sound_exit(i,j+1) = refpropm('A','P',Pressure_exit,'S',Inlet_entropy,Fluid{i}, refpr
                h_static_exit(i,j+1) = refpropm('H','P',Pressure_exit,'S',Inlet_entropy,Fluid{i}, re
```

```
62                  visc_exit(i,j+1) = refpropm('V','P',Pressure_exit,'S',Inlet_entropy,Fluid{i}, refpropdir);
63                  mach_exit(i,j+1) = sqrt(2*(h_inlet(i,j+1)-h_static_exit(i,j+1))/sound_exit(i,j+1)^2);       % Co
64              end
65
66              %% Calculation of the mass flow rate into the tank(s)
67
68              rho_exit(i,j+1) = refpropm('D','P',Pressure_exit,'S',Inlet_entropy,Fluid{i}, refpropdir);
69              vel_exit(i,j+1) = mach_exit(i,j+1)*sound_exit(i,j+1);                                          % Calcul
70              Re_exit_isentropic(i,j+1) = rho_exit(i,j+1) *d_inlet*vel_exit(i,j+1)/visc_exit(i,j+1);         % Calcul
71              cd(i,j+1) =  I + J/(Re_exit_isentropic(i,j+1)^(0.25));                                         % Calcul
72              mfr(i,j+1) = cd(i,j+1)*rho_exit(i,j+1)*vel_exit(i,j+1)*A_inlet;                                % Calcul
73              Re_entrance_actual(i,j+1)= 4*mfr(i,j+1)/(pi*d_inlet*visc_exit(i,j+1));                         % Calcul
74              dM_inlet = mfr(i,j+1)*dt;                                                                      % Amount
75          end
76
77          %% Heat transfer calculations & caluclations of the thermodynamic properties of the gas in the tank(s) w
78          if l_d(i) <= 3 | blnOneZone{i} == 1
79
80              Nus(i,j+1) =   a_1*Re_entrance_actual(i,j+1)^(b_1);                  % Nusselt number and Reynolds
81              k_gas(i,j+1) = refpropm('L','T',Temp_gas(i,j),'P',P_gas(i,j),Fluid{i}, refpropdir);  % Thermal condu
82              heat_coef_forced(i,j+1) = Nus(i,j+1)*k_gas(i,j+1)/d_tank(i);         % Calculation of the heat tran
83
84              if Inner_wall_boundary(i) == 1
85                  Qsurf(i,j+1) = -dt*surf_area(i)*heat_coef_forced(i,j+1)*(Temp_gas(i,j)-Inner_temp_wall_isotherma
86              else
87                  Qsurf(i,j+1) = -dt*surf_area(i)*heat_coef_forced(i,j+1)*(Temp_gas(i,j)-Temp_wall{i}(1,j));
88                  Temp_wall{i}(1,j+1) = Temp_wall{i}(1,j)+ CFL_liner(i)*(Temp_wall{i}(2,j)- Temp_wall{i}(1,j) - Qs
89
90                  if Outer_wall_boundary(i)==1
91                      Temp_wall{i}(number_of_gridpoints(i),j+1) = Outer_temp_wall_isothermal(i);
92                  else
93                      Temp_wall{i}(number_of_gridpoints(i),j+1) = Temp_wall{i}(number_of_gridpoints(i),j)+2*CFL_la
94                  end
95                  % Computation of the temperature of the struture of the tank(s)
96                  for k=2:number_of_gridpoints(i)-1
97                      if (k>=2)&&(k<=int_pt_liner_laminate(i)-1)
98                          Temp_wall{i}(k,j+1) = Temp_wall{i}(k,j)+CFL_liner(i)*(Temp_wall{i}(k+1,j)-2*Temp_wall{i}
99                      elseif (k>=int_pt_liner_laminate(i)+1)&&(k<=number_of_gridpoints(i)-1)
100                         Temp_wall{i}(k,j+1) = Temp_wall{i}(k,j)+CFL_laminate(i)*(Temp_wall{i}(k+1,j)-2*Temp_wall
101                     else
102                         Temp_wall{i}(k,j+1) = (cond_laminate(i)*(Temp_wall{i}(k+1,j)+CFL_laminate(i)*(Temp_wall+
103                     end
104                 end
105             end
106             m_gas(i,j+1) = m_gas(i,j)+ dM_inlet;                                                  % Mass of gas in
107             Ugas(i,j+1)=Ugas(i,j)+Qsurf(i,j+1)+h_inlet(i,j+1)*dM_inlet;                           % Internal energy
108             u_gas(i,j+1)= Ugas(i,j+1)/m_gas(i,j+1);                                               % Specific energy
109             rho_gas(i,j+1)=m_gas(i,j+1)/vol_tank(i);                                              % Density of the
110             P_gas(i,j+1) = refpropm('P','D',rho_gas(i,j+1),'U',u_gas(i,j+1),Fluid{i}, refpropdir);          %
111             Temp_gas(i,j+1) = refpropm('T','D',rho_gas(i,j+1),'U',u_gas(i,j+1),Fluid{i}, refpropdir);       %
112
113         else
114             Re_compression(i,j+1) = Re_entrance_actual(i,j+1)*(d_inlet/d_tank(i));                % Reynolds number
115
116             Nus_zone1{i}(j+1) =  a_1*Re_entrance_actual(i,j+1)^(b_1);                             % Nusselt number
117             Nus_zone2{i}(j+1) =  c_1*Re_compression(i,j+1)^(d_1);                                 % Nusselt number
118
119             k_gas_zone1{i}(j+1) =  refpropm('L','T',Temp_gas_zone1{i}(j),'P',P_gas_zone1{i}(j),Fluid{i}, refprop
120             k_gas_zone2{i}(j+1) =  refpropm('L','T',Temp_gas_zone2{i}(j),'P',P_gas_zone2{i}(j),Fluid{i}, refprop
121
122             heat_coef_forced_zone1{i}(j+1) =  Nus_zone1{i}(j+1)*k_gas_zone1{i}(j+1)/d_tank(i);            %
123             heat_coef_forced_zone2{i}(j+1) =  Nus_zone2{i}(j+1)*k_gas_zone2{i}(j+1)/l_zone2_total(i);     %
124
125             % Step 1. Equating the respecting values of zone 1 and zone 2 to
126             % matrices with 'similar' names
127
```

```
128             Vgas(1)=volume_zone1(i);
129             Vgas(2)=volume_zone2(i);
130             Mgas(1)=m_gas_zone1{i}(j);
131             Mgas(2)=m_gas_zone2{i}(j);
132             Ugas_twozone(1)=u_gas_zone1{i}(j)*Mgas(1);
133             Ugas_twozone(2)=u_gas_zone2{i}(j)*Mgas(2);
134             Asurf(1)=surface_area_zone1(i);
135             Asurf(2)=surface_area_zone2(i);
136             Tgas(1)=Temp_gas_zone1{i}(j);
137             Tgas(2)=Temp_gas_zone2{i}(j);
138             if Inner_wall_boundary(i) == 1
139                 Twall(1,1)=Inner_temp_wall_isothermal(i);
140                 Twall(2,1)=Inner_temp_wall_isothermal(i);
141             else
142                 Twall(1,1)=Temp_wall_zone1{i}(1,j);
143                 Twall(2,1)=Temp_wall_zone2{i}(1,j);
144             end
145             % Step 2: apply the change of internal energy due to heat transfer and mass
146             % input through nozzle:
147
148             dM_inlet = mfr(i,j+1)*dt;
149
150             Qsurf(1)=- dt*Asurf(1)*(heat_coef_forced_zone1{i}(j+1))*(Tgas(1)-Twall(1,1));
151             Qsurf(2)=- dt*Asurf(2)*(heat_coef_forced_zone2{i}(j+1))*(Tgas(2)-Twall(2,1));
152
153             Ugas_twozone(1)=Ugas_twozone(1)+Qsurf(1)+h_inlet(i,j+1)*dM_inlet;
154             Ugas_twozone(2)=Ugas_twozone(2)+Qsurf(2);
155
156             Mgas(1)=Mgas(1)+dM_inlet;
157             Mgas(2)=Mgas(2);
158
159             for m=1:2
160                 hgas(m)=refpropm('H','D',Mgas(m)/Vgas(m),'U',Ugas_twozone(m)/Mgas(m),Fluid{i}, refpr
161             end
162
163
164             % Step 2: Find the amount of mass that needs to be transferred from zone 1
165             % to zone 2 to equalise their pressure
166             % (we assume forward Euler integration, therefore we use the specific
167             % enthalpies h from the start of the timestep. We provide enthalpies for
168             % both zones in case the flow gets reversed).
169
170             dM_guess = dM_inlet*(volume_zone2(i)/(volume_zone1(i)+volume_zone2(i))) ;
171             dM_12 = find_dM_12(hgas,Vgas,Mgas,Ugas_twozone,Fluid{i},dM_guess, refpropdir);
172
173             % Step 3: Apply this change to the mass and update all properties:
174
175             m_gas_zone1{i}(j+1)=Mgas(1)-dM_12;
176             m_gas_zone2{i}(j+1)=Mgas(2)+dM_12;
177
178             u_gas_zone1{i}(j+1)=(Ugas_twozone(1)-max(0,dM_12)*hgas(1)-min(0,dM_12)*hgas(2))/m_gas_zo
179             u_gas_zone2{i}(j+1)=(Ugas_twozone(2)+max(0,dM_12)*hgas(1)+min(0,dM_12)*hgas(2))/m_gas_zo
180
181             rho_gas_zone1{i}(j+1)=m_gas_zone1{i}(j+1)/volume_zone1(i);
182             rho_gas_zone2{i}(j+1)=m_gas_zone2{i}(j+1)/volume_zone2(i);
183
184             Temp_gas_zone1{i}(j+1)=refpropm('T','D',rho_gas_zone1{i}(j+1),'U', u_gas_zone1{i}(j+1),F
185             Temp_gas_zone2{i}(j+1)=refpropm('T','D',rho_gas_zone2{i}(j+1),'U', u_gas_zone2{i}(j+1),F
186
187             P_gas_zone1{i}(j+1)=refpropm('P','D',rho_gas_zone1{i}(j+1),'U', u_gas_zone1{i}(j+1),Flui
188             P_gas_zone2{i}(j+1)=refpropm('P','D',rho_gas_zone2{i}(j+1),'U', u_gas_zone2{i}(j+1),Flui
189
190             m_gas(i,j+1) = m_gas_zone1{i}(j+1) + m_gas_zone2{i}(j+1);
191             rho_gas(i,j+1) = m_gas(i,j+1)/vol_tank(i);
192             u_gas(i,j+1)= (u_gas_zone1{i}(j+1)*m_gas_zone1{i}(j+1)+ u_gas_zone2{i}(j+1)*m_gas_zone2{
193             Ugas(i,j+1) = u_gas(i,j+1)*m_gas(i,j+1);
```

```
194             Temp_gas(i,j+1)  = refpropm('T','D',rho_gas(i,j+1),'U',u_gas(i,j+1),Fluid{i}, refpropdir);
195             P_gas(i,j+1)  = refpropm('P','D',rho_gas(i,j+1),'U',u_gas(i,j+1),Fluid{i}, refpropdir);
196
197             if Inner_wall_boundary(i) == 1
198                 Qsurf_zone1{i}(j+1) = -dt*surface_area_zone1(i)* heat_coef_forced_zone1{i}(j+1)*(Temp_gas_zone1
199                 Qsurf_zone2{i}(j+1) = -dt*surface_area_zone2(i)* heat_coef_forced_zone2{i}(j+1)*(Temp_gas_zone2
200             else
201                 Qsurf_zone1{i}(j+1) = -dt*surface_area_zone1(i)* heat_coef_forced_zone1{i}(j+1)*(Temp_gas_zone1
202                 Qsurf_zone2{i}(j+1) = -dt*surface_area_zone2(i)* heat_coef_forced_zone2{i}(j+1)*(Temp_gas_zone2
203
204                 Temp_wall_zone1{i}(1,j+1) = Temp_wall_zone1{i}(1,j)+ CFL_liner(i)*(Temp_wall_zone1{i}(2,j)- Temp
205                 Temp_wall_zone2{i}(1,j+1) = Temp_wall_zone2{i}(1,j)+ CFL_liner(i)*(Temp_wall_zone2{i}(2,j)- Temp
206
207                 if Outer_wall_boundary(i)==1
208                     Temp_wall_zone1{i}(number_of_gridpoints(i),j+1) = Outer_temp_wall_isothermal(i);
209                     Temp_wall_zone2{i}(number_of_gridpoints(i),j+1) = Outer_temp_wall_isothermal(i);
210                 else
211                     Temp_wall_zone1{i}(number_of_gridpoints(i),j+1) = Temp_wall_zone1{i}(number_of_gridpoints(i)
212                     Temp_wall_zone2{i}(number_of_gridpoints(i),j+1) = Temp_wall_zone2{i}(number_of_gridpoints(i)
213                 end
214                 % Computation of the temperature of the struture of the tank(s)
215                 for k=2:number_of_gridpoints(i)-1
216                     if (k>=2)&&(k<=int_pt_liner_laminate(i)-1)
217                         Temp_wall_zone1{i}(k,j+1) = Temp_wall_zone1{i}(k,j)+CFL_liner(i)*(Temp_wall_zone1{i}(k+1
218                         Temp_wall_zone2{i}(k,j+1) = Temp_wall_zone2{i}(k,j)+CFL_liner(i)*(Temp_wall_zone2{i}(k+1
219                     elseif (k>=int_pt_liner_laminate(i)+1)&&(k<=number_of_gridpoints(i)-1)
220                         Temp_wall_zone1{i}(k,j+1) = Temp_wall_zone1{i}(k,j)+CFL_laminate(i)*(Temp_wall_zone1{i}(
221                         Temp_wall_zone2{i}(k,j+1) = Temp_wall_zone2{i}(k,j)+CFL_laminate(i)*(Temp_wall_zone2{i}(
222                     else
223                         Temp_wall_zone1{i}(k,j+1) = (cond_laminate(i)*(Temp_wall_zone1{i}(k+1,j)+CFL_laminate(i)
224                         Temp_wall_zone2{i}(k,j+1) = (cond_laminate(i)*(Temp_wall_zone2{i}(k+1,j)+CFL_laminate(i)
225                     end
226                 end
227             end
228
229         end
230
231     end
232 end
```

References

[1] C. Dicken and W. Mérida, "Measured effects of filling time and initial mass on the temperature distribution within a hydrogen cylinder during refuelling", *Journal of power sources*, vol. 165, no. 1, pp. 324–336, Feb. 2007, ISSN: 03787753. DOI: 10.1016/j.jpowsour.2006.11.077. [Online]. Available: https://www.engineeringvillage.com/share/document.url?mid=cpx%7B%5C_%7D30c221110dfeaa71cM69f92061377553%7B%5C&%7Ddatabase=cpx.

[2] J. Zheng, J. Guo, J. Yang, Y. Zhao, L. Zhao, X. Pan, J. Ma, and L. Zhang, "Experimental and numerical study on temperature rise within a 70 MPa type III cylinder during fast refueling", *International journal of hydrogen energy*, vol. 38, no. 25, pp. 10 956–10 962, Aug. 2013, ISSN: 0360-3199. DOI: 10.1016/J.IJHYDENE.2013.02.053. [Online]. Available: https://www.sciencedirect.com/science/article/pii/S0360319913004199?via%7B%5C%%7D3Dihub.

[3] P. L. Woodfield, M. Monde, and T. Takano, "Heat Transfer Characteristics for Practical Hydrogen Pressure Vessels Being Filled at High Pressure", *Journal of thermal science and technology*, vol. 3, no. 2, pp. 241–253, 2008. DOI: 10.1299/jtst.3.241.

[4] C. J. B. Dicken and W. Mérida, "Modeling the Transient Temperature Distribution within a Hydrogen Cylinder during Refueling", *Numerical heat transfer, part a: Applications*, vol. 53, no. 7, pp. 685–708, Nov. 2007, ISSN: 1040-7782. DOI: 10.1080/10407780701634383. [Online]. Available: http://www.tandfonline.com/doi/abs/10.1080/10407780701634383

[5] Y. Zhao, G. Liu, Y. Liu, J. Zheng, Y. Chen, L. Zhao, J. Guo, and Y. He, "Numerical study on fast filling of 70 MPa type III cylinder for hydrogen vehicle", *International journal of hydrogen energy*, vol. 37, no. 22, pp. 17 517–17 522, 2012, ISSN: 0360-3199. DOI: https://doi.org/10.1016/j.ijhydene.2012.03.046. [Online]. Available: http://www.sciencedirect.com/science/article/pii/S0360319912006477.

[6] B. I. Lee and M. G. Kesler, "A generalized thermodynamic correlation based on three-parameter corresponding states", *Aiche journal*, vol. 21, no. 3, pp. 510–527, May 1975, ISSN: 0001-1541. DOI: 10.1002/aic.690210313. [Online]. Available: http://doi.wiley.com/10.1002/aic.690210313.

[7] M. Monde, Y. Mitsutake, P. L. Woodfield, and S. Maruyama, "Characteristics of heat transfer and temperature rise of hydrogen during rapid hydrogen filling at high pressure", *Heat transfer - asian research*, vol. 36, no. 1, pp. 13–27, Jan. 2007, ISSN: 10992871. DOI: 10.1002/htj.20140. [Online]. Available: http://doi.wiley.com/10.1002/htj.20140.

[8] S. B. Pope, *Turbulent Flows*. Cambridge University Press, 2000, ISBN: 9780521598866. [Online]. Available: https://books.google.co.uk/books?id=HZsTw9SMx-0C.

[9] H. J. Hussein, S. P. Capp, and W. K. George, "Velocity measurements in a high-Reynolds-number, momentum-conserving, axisymmetric, turbulent jet", *Journal of fluid mechanics*, vol. 258, no. -1, p. 31, Jan. 1994, ISSN: 0022-1120. DOI: 10.1017/S002211209400323X. [Online]. Available: http://www.journals.cambridge.org/abstract%7B%5C_%7DS002211209400323X.

[10] E. W. Lemmon, M. L. Huber, and M. O. McLinden, *NIST Standard Reference Database 23: Reference Fluid Thermodynamic and Transport Properties-REFPROP, Version 9.1, National Institute of Standards and Technology*, 2013. DOI: http://dx.doi.org/10.18434/T4JS3C. [Online]. Available: https://www.nist.gov/srd/refprop.

[11] F. P. Incropera, *Fundamentals of heat and mass transfer*, ser. Fundamentals of Heat and Mass Transfer v. 1. John Wiley, 2007, ISBN: 9780471457282. [Online]. Available: https://books.google.co.uk/books?id=%7B%5C_%7DP9QAAAAMAAJ.

[12] S. Kakaç, R. K. Shah, and W. Aung, *Handbook of single-phase convective heat transfer*, ser. A Wiley Interscience publication. Wiley, 1987, ISBN: 9780471817024. [Online]. Available: https://books.google.co.uk/books?id=FCJRAAAAMAAJ.